FARADAY

Mechanistic and kinetic study of formaldehyde production in the atmospheric oxidation of dimethyl sulfide

Shawn P. Urbanski,[a] Robert E. Stickel,[b] Zhizhong Zhao,[a] and Paul H. Wine[a,b,c]*

[a] *School of Earth and Atmospheric Sciences,* [b] *Georgia Tech Research Institute,* [c] *School of Chemistry and Biochemistry, Georgia Institute of Technology, Atlanta, GA 30332, USA*

Tunable diode laser spectroscopic detection of formaldehyde (H_2CO) and HCl coupled with laser flash photolysis of Cl_2CO–CH_3SCH_3–O_2–N_2 mixtures, in both the presence and absence of NO, has been utilized to conduct a mechanistic and kinetic investigation of the atmospheric oxidation of the CH_3SCH_2 radical, a product of dimethyl sulfide (DMS, CH_3SCH_3) reactions with OH and NO_3 in the atmosphere. The temperature dependence of the $CH_3SCH_2O_2$ + NO rate coefficient (k_2) and the 298 K rate coefficient for the $CH_3SCH_2O_2$ self reaction (k_4) have been measured. The Arrhenius expression $k_2 = 4.9 \times 10^{-12}$ exp(263/T) cm^3 molecule^{-1} s^{-1} adequately summarizes our $CH_3SCH_2O_2$ + NO kinetic data over the temperature range 261–400 K. Contributions from side reactions, which are not completely quantifiable, limit the accuracy of the k_4 (298 K) determination; our results indicate that the true value for this rate coefficient is within the range $(1.2 \pm 0.5) \times 10^{-11}$ cm^3 molecule^{-1} s^{-1}. In both reactions $CH_3SCH_2O_2$ is converted to H_2CO with unit yield (at T = 298 K). Our results demonstrate that the lifetime of CH_3SCH_2O, a proposed precursor to H_2CO, is less than 30 μs at 261 K and 10 Torr total pressure.

Significant interest exists in the atmospheric fate of DMS. It is produced by the biological activity of phytoplankton in the surface ocean[1] and its release from the oceans is the largest natural source of atmospheric sulfur, constituting an estimated 60% of biogenic emissions.[1–3] The oxidation of DMS in the troposphere may play an important role in the global climate system because sulfuric acid is a potential oxidation product. It has been proposed that, through the production of sulfuric acid, DMS may impact aerosol production and cloud formation processes, and hence the earth's radiation budget.[4,5] An unravelling of the complex DMS oxidation mechanism, through determination of the reaction rates and stable product yields for the range of relevant environmental conditions, is necessary for an accurate assessment of the role DMS plays in the global climate system.

Reaction with the hydroxyl radical in the daytime and the nitrate radical during the night are believed to be the dominant processes initiating the oxidation of DMS in the atmosphere.[1,6] The reaction of DMS with OH proceeds *via* both O_2-dependent and O_2-independent pathways, with the O_2-independent pathway accounting for 75% of the overall reactivity at 300 K.[7] The O_2-dependent pathway involves the formation of an adduct and the subsequent competition between adduct reaction with O_2 and adduct decomposition to reform DMS and OH.[7–9] The O_2-independent pathway is dominated by H-atom abstraction, producing the CH_3SCH_2 radical.[10,11] By analogy with other alkyl radical oxidation processes, the following mechanism has been proposed for the atmospheric oxidation of the CH_3SCH_2 radical:[12]

$$CH_3SCH_2 + O_2 + M \rightarrow CH_3SCH_2O_2 + M \quad (1)$$

$$CH_3SCH_2O_2 + NO \rightarrow CH_3SCH_2O + NO_2 \quad (2)$$

$$CH_3SCH_2O + M \rightarrow H_2CO + CH_3S + M \quad (3)$$

Recent laboratory investigations have confirmed the occurrence of reactions (1)–(3).[11,13,14] Utilizing pulse radiolysis in conjunction with time-resolved UV absorption spectroscopy, Wallington *et al.*[13] observed NO_2 production from reaction (2) and measured an NO_2 yield of 0.81 ± 0.15, as well as a room-temperature rate coefficient of $(1.9 \pm 0.6) \times 10^{-11}$ cm^3 molecule^{-1} s^{-1}; these investigators also reported a room-temperature rate coefficient for reaction (1) of $(5.7 \pm 0.4) \times 10^{-12}$ cm^3 molecule^{-1} s^{-1} in 750 Torr SF_6. Experiments exploring the reaction of DMS with NO_3 in reaction mixtures containing O_2 have been interpreted as demonstrating H_2CO and CH_3S formation from the decomposition of the CH_3SCH_2O intermediate.[14] More recently, laser flash photolysis (LFP)–pulsed laser-induced fluorescence (PLIF) studies investigating the chemistry of the DMS + OH + O_2 + NO system have provided evidence that CH_3S is the dominant sulfur-containing product generated by the sequence of reactions (1)–(3).[11] The CH_3S radical is a central species in current proposed DMS oxidation mechanisms because it is theorized to be the principal source of the frequently cited DMS oxidation products SO_2, SO_3, methane sulfonic acid (MSA), and sulfuric acid.[1] Consequently, much attention has been devoted to the chemistry of CH_3S. However, until quite recently, comparatively little effort has been expended towards establishing quantitatively which chemical processes actually produce CH_3S.

In this paper we report the results of a mechanistic and kinetic study of the conversion of CH_3SCH_2 to formaldehyde in the presence of O_2, and in the presence and absence of NO. We obtain H_2CO yield information as well as kinetic information for reaction (2) and for the $CH_3SCH_2O_2$ self-reaction:

$$CH_3SCH_2O_2 + CH_3SCH_2O_2 \rightarrow CH_3SCH_2O + CH_3SCH_2O + O_2 \quad (4a)$$

$$CH_3SCH_2O_2 + CH_3SCH_2O_2 \rightarrow CH_3SCH_2OH + CH_3SCHO + O_2 \quad (4b)$$

The $CH_3SCH_2O_2$ self-reaction is of interest for two reasons. In the remote marine boundary layer, NO concentrations are typically very low, *i.e.* <10 pptv,[15,16] and reaction with HO_2 may loom large in the overall fate of $CH_3SCH_2O_2$. Therefore, knowledge of the rate coefficient for the reaction of $CH_3SCH_2O_2$ with HO_2 is of great importance for understanding the atmospheric fate of DMS. This radical–radical reaction presents many experimental and technical challenges. Detailed understanding of the kinetics and mechanism of the $CH_3SCH_2O_2$ self-reaction is a prerequisite for obtaining accurate kinetic information regarding the $CH_3SCH_2O_2$ + HO_2 reaction. Also, depending on the kinetics of the $CH_3SCH_2O_2$ + HO_2 reaction, the $CH_3SCH_2O_2$ self-reaction may be

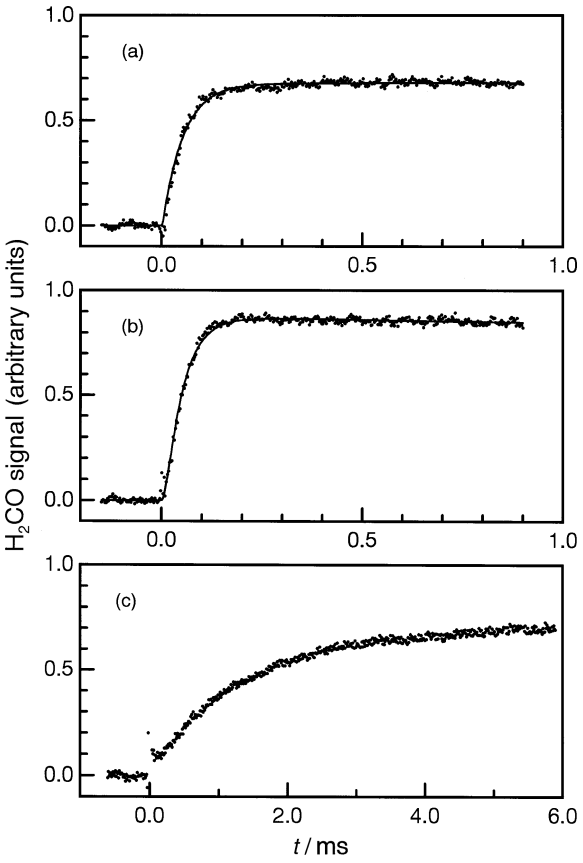

Fig. 1 Typical H_2CO appearance temporal profiles observed following 248 nm laser flash photolysis of Cl_2CO in the presence of O_2, DMS or CH_3OH, NO (in some experiments) and 10 Torr N_2 at 298 K. Laser fluence of *ca.* 15 mJ cm^{-2} $pulse^{-1}$, 32 excimer laser flashes averaged. Concentrations in units of 10^{13} cm^{-3} are (a) 300 DMS + 10 500 O_2 + 170 NO + 1.2 Cl at $t = 0$; (b) 98 CH_3OH + 10 500 O_2 + 1.2 Cl at $t = 0$; (c) 280 DMS + 2500 O_2 + 3.0 Cl at $t = 0$.

important in its own right under certain remote marine boundary layer conditions.

Experimental

The LFP–time-resolved tunable diode laser absorption spectroscopy (TDLAS) technique used in this study was similar to that used in a number of previous studies of DMS oxidation carried out in our laboratory.[10,17,18] Laser flash photolysis of phosgene (Cl_2CO) at 248 nm was used to produce chlorine atoms in the presence of DMS, O_2 and, in some cases, NO. The very fast reaction of Cl with DMS then produced CH_3SCH_2 radicals with a yield measured in a previous study.[17] The CH_3SCH_2 radicals then underwent an addition reaction with O_2 producing $CH_3SCH_2O_2$ peroxyl radicals. Finally, the peroxyl radicals reacted either with NO or with themselves to produce H_2CO (either directly or *via* the intermediate CH_3SCH_2O). A small fraction of the DMS was also photolyzed by the 248 nm flash. The effect of the DMS photoproducts, CH_3S and CH_3,[19] was not significant in the NO experiments but was apparent in the experiments without NO. Corrections for this effect are described below.

The LFP–TDLAS apparatus has been described in detail elsewhere.[10,17] Only a brief description, including features unique to the present study, is included here. The IR probe was provided by a lead-salt diode laser in a helium-refrigerated cryostat. A KrF excimer laser produced pulses of 248 nm photolysis light with an energy density in the reaction cell of *ca.* 15–30 mJ cm^{-2} and a duration of *ca.* 20 ns.

For the experiments with NO, the diode laser was tuned to an isolated H_2CO line at 2863.32 cm^{-1} and modulated by a

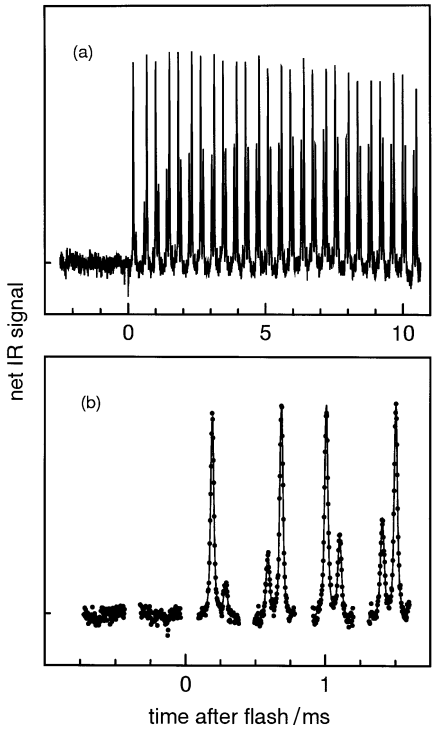

Fig. 2 Illustrations of the simultaneous detection of HCl and H_2CO formed in the Cl + DMS + O_2 system. Experimental conditions: $T = 298$ K; $P = 20$ Torr N_2; concentrations in units of 10^{13} molecule cm^{-3} are 960 DMS + 24 000 O_2 + 5.0 Cl at $t = 0$; laser fluence 34 mJ cm^{-2} $pulse^{-1}$; 32 excimer laser flashes averaged. (a) Entire raw data set. (b) Expanded view of three modulation cycles around the photolysis flash including the raw data as dots and the best-fit Voigt profiles as smooth curves.

40 KHz sine-wave signal adjusted in amplitude for optimum second harmonic detection of the absorption signal. The H_2CO concentration was recovered from the digitized IR signal by subsequent computation of the second harmonic Fourier amplitude in a few hundred intervals, each one a single modulation cycle in duration. Calibration of the IR H_2CO absorption signal was obtained from back-to-back experiments with methanol (CH_3OH) replacing DMS as the Cl reaction partner. The reactions:

$$Cl + CH_3OH \rightarrow HCl + CH_2OH \quad (5)$$

$$CH_2OH + O_2 \rightarrow HO_2 + H_2CO \quad (6)$$

are known to produce formaldehyde with unit yield[20] and the time dependence of the H_2CO absorption signal was similar to that observed in the DMS experiments, so that the comparison was straightforward [see Fig. 1(a) and 1(b)].

In experiments performed without NO, the observed formaldehyde formation rate was much slower and appeared to follow second-order kinetics [see Fig. 1(c)]. The different, *i.e.* non-exponential, appearance temporal profile made reliable comparison of this signal with methanol results much more difficult. Thus a different approach was adopted to measure the yield of H_2CO from reaction (4). A near-coincidence of H_2CO and HCl absorption lines at 2863.0 cm^{-1} was exploited to monitor both species simultaneously. For these experiments, the diode laser was modulated over both lines by a 1.2 kHz symmetric triangle waveform. The resulting signal was analyzed by fitting each half cycle to a function including two Voigt profiles and a polynomial background as shown in Fig. 2. Methanol experiments were used to determine the HCl to H_2CO signal ratio under unit yield conditions. Because CH_3SCH_2 radicals are produced one-for-one with HCl in the initial H-abstraction step and rapidly add oxygen to form $CH_3SCH_2O_2$, the HCl absorption signal provided an *in situ*

calibration for measurement of the H_2CO yield from reaction (4). Calibration of the HCl absorption signal was achieved by standard addition of HCl. The accuracy of the HCl standard addition calibration was verified by measuring the HCl yield from the reaction $Cl + C_2H_6$, a thoroughly studied reaction with a known HCl yield of unity.[21] The slower modulation speed in the experiments without NO was necessary to achieve sufficient definition of the absorption spectrum for the line shape analysis. Fortunately, the resulting slower response was acceptable owing to the slower H_2CO formation rate.

The pure gases used in this study were obtained from Air Products Specialty Gases (N_2, O_2), Matheson Gas Products (Cl_2CO, NO, HCl) and Spectra Gases (C_2H_6) and had the following stated minimum purities: N_2, 99.999%; O_2, 99.994%; Cl_2CO, 99.0%; NO, 99.0%; HCl, 99.0%; C_2H_6, 99.97%. The N_2 and O_2 were used as supplied, while the Cl_2CO, NO, HCl and C_2H_6 were degassed at 77 K prior to use. The dimethyl sulfide was acquired from Aldrich Chemical Corp. and had a minimum stated purity of 99.0%. The dimethyl sulfide was transferred under nitrogen into vials fitted with high-vacuum stopcocks. The methanol, minimum stated purity 99.9%, was obtained from Fisher Scientific. Both the dimethyl sulfide and the methanol were degassed repeatedly at 77 K before use.

Results and Discussion

$CH_3SCH_2O_2 + NO$

With NO in the system, the formation of H_2CO was observed to be pseudo-first order with a rate proportional to the NO concentration. This linear relationship held up to the fastest appearance rate measured (*ca.* 35 000 s^{-1}) indicating that the $CH_3SCH_2O_2 + NO$ reaction is the rate-limiting step in generating formaldehyde under all experimental conditions investigated; hence, the lifetime of CH_3SCH_2O toward decomposition to formaldehyde under these conditions is less than 30 μs. Furthermore, the H_2CO appearance rate was independent of $[O_2]$ (for $[O_2] > 2 \times 10^{15}$ molecule cm^{-3}), $[CH_3SCH_2]_0$, and total pressure, suggesting that formation of H_2CO by NO-independent channels was not significant in these experiments. It has been suggested that CH_3SCH_2O reacts with O_2 producing CH_3SCHO and HO_2;[14] the invariance of both the H_2CO appearance rate and the H_2CO IR signal strength to variations in $[O_2]$ over a range of 2×10^{15} to 3×10^{17} molecule cm^{-3} demonstrates that this reaction was not significant under our experimental conditions. This is true for experiments conducted in both the absence and the presence of NO. Likewise, Turnipseed *et al.*[11] did not observe evidence of HO_2 production , which would have manifested itself as OH regeneration, in their LFP–PLIF examination of the OH + DMS reaction in the presence of O_2 and NO. Linear least-squares fits to plots of the pseudo-first-order H_2CO appearance rate against [NO] are shown in Fig. 3 for three of the six temperatures studied. An Arrhenius plot for the $CH_3SCH_2O_2 + NO$ reaction is shown in Fig. 4; the rate coefficient for reaction (2) is found to decrease slightly with increasing temperature leading to the Arrhenius expression: $k_2 = (4.9 \times 10^{-12})$ exp(263/T) cm^3 $molecule^{-1}$ s^{-1} for $261 \leqslant T/K \leqslant 400$ K. Relative uncertainties (95% confidence limit) in the A factor and activation temperature are 25 and 50%, respectively.

The yield of H_2CO in the presence of NO was determined by taking ratios of the results observed in the DMS system and the methanol reference mixture, and correcting these ratios for minor variations in initial conditions. The yields from the DMS system were also corrected for the known pressure-dependent abstraction branching ratio of the Cl + DMS reaction.[17] At 298 K and 10 Torr total pressure, 17 experiments were conducted with reagent concentrations

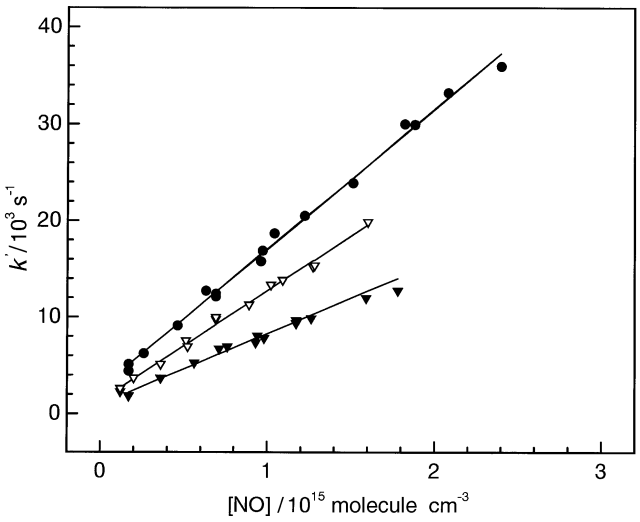

Fig. 3 Pseudo-first-order rate coefficient *versus* [NO] for the reaction $CH_3SCH_2O_2 + NO$ at temperatures of (●) 260, (▽) 298 and (▼) 400 K. Symbols are experimental data. Lines are linear least-squares fits. Best-fit slopes are, in units of 10^{-11} cm^3 $molecule^{-1}$ s^{-1}, 1.45 ± 0.05 at 260 K, 1.14 ± 0.05 at 298 K and 0.73 ± 0.06 at 400 K; uncertainties are 2σ and represent precision only.

varied as follows (units are 10^{13} molecule cm^{-3}): DMS, 322–526; CH_3OH, 140–301; Cl_2CO, 321–699; Cl at t = 0, 1.0–2.7; O_2, 21 500–28 000; NO, 37–135. The H_2CO yield from reaction (2) was found to be 1.04 with a 2σ uncertainty of 0.13 when considering precision only. The overall yield was measured at other temperatures and appeared to be close to unity; however, these results could not be reduced to quantitative yields for reaction (2) alone since the CH_3SCH_2 yield from the Cl + DMS reaction has not been measured quantitatively at temperatures other than 298 K. Our result, in conjunction with the recent study of Turnipseed *et al.*,[11] confirms speculation that CH_3S and H_2CO are produced with essentially unit yield from the $CH_3SCH_2O_2 + NO$ reaction.

Our kinetic and mechanistic studies of the $CH_3SCH_2O_2 + NO$ reaction have determined the temperature dependence of the rate coefficient from 261 to 400 K and established that H_2CO and CH_3S are produced in near unit yield *via* the short-lived intermediate CH_3SCH_2O (lifetime < 30 μs at 261 K and 10 Torr total pressure). To our knowledge, the temperature dependence of reaction (2) presented in this study is the first to be reported in the literature. The room-temperature rate coefficient reported here may be regarded as

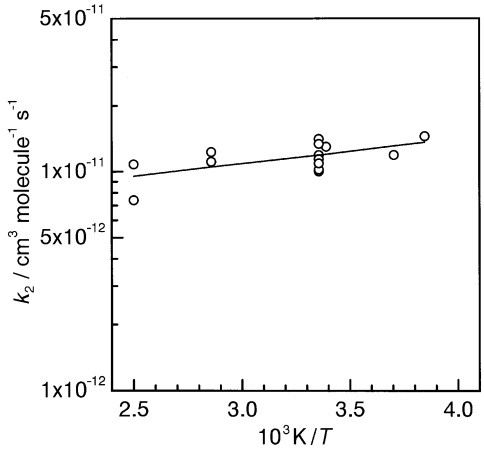

Fig. 4 Arrhenius plot for the $CH_3SCH_2O_2 + NO$ reaction [reaction (2)]. Solid line is obtained from a least-squares analysis and gives the Arrhenius expression $k_2(T) = 4.93 \times 10^{-12}$ exp[263/T] cm^3 $molecule^{-1}$ s^{-1}.

being in agreement with the two previous room-temperature measurements of Wallington *et al.*[13] and Turnipseed *et al.*,[11] but is considerably more precise than either previous measurement. Using a pulse radiolysis-time resolved UV absorption technique, Wallington *et al.*[13] obtained a room-temperature value of $(1.9 \pm 0.6) \times 10^{-11}$ cm^3 molecule^{-1} s^{-1} in 750 Torr of SF_6. This result is a factor of 1.6 faster than our 298 K value, although the two results agree within the combined experimental uncertainties. In the Wallington *et al.*[13] study, the chemical scheme prohibited use of very high O_2 levels. As a result, the pseudo-first-order rate of $CH_3SCH_2O_2$ appearance could not be made much faster than the pseudo-first-order rate of $CH_3SCH_2O_2$ loss *via* reaction with NO. This limitation, which did not affect our study, increased the uncertainty in the earlier result. From analysis of CH_3S temporal profiles, Turnipseed *et al.*[11] estimate a room temperature rate coefficient for reaction (2) of $(8.0 \pm 3.1) \times 10^{-12}$ cm^3 molecule^{-1} s^{-1} in 22 Torr of O_2; given the rather large reported uncertainty in this rate coefficient, it may also be considered consistent with our measurement. The temperature dependence determined in the present study demonstrates that, like the CH_3O_2 + NO reaction, the $CH_3SCH_2O_2$ + NO reaction possesses a small, negative activation energy.[22–24] Furthermore, the room-temperature rate coefficient is similar in magnitude to the well established room-temperature rate coefficients for several other peroxyl radical reactions with NO.[22–24]

The H_2CO yield measurement presented in the current study, combined with the approximate unit yield of NO_2 reported by Wallington *et al.*[13] and the approximate unit yield of CH_3S reported by Turnipseed *et al.*,[11] verify the mechanism for CH_3SCH_2 oxidation in the presence of O_2 and NO discussed in the introductory section.

$CH_3SCH_2O_2 + CH_3SCH_2O_2$

As mentioned earlier, the more complicated kinetics of H_2CO formation in the absence of NO made comparison of the NO-free results with the methanol reference system much less reliable. For these experiments, HCl and H_2CO were monitored simultaneously, and initially using the kinetic model summarized in Table 1, the FACSIMILE[25] program, a combination numerical integration and non-linear least-squares fit routine, was employed to adjust the rate coefficient k_4 (defined by $d[CH_3SCH_2O_2]/dt = 2k_4[CH_3SCH_2O_2]^2$) and the H_2CO yield from reaction (4), Φ(4a), to fit the observed concentration profiles. As mentioned previously, both the H_2CO appearance rate and the H_2CO IR absorption signal were independent of O_2 concentration (for $[O_2] > 2 \times 10^{15}$ molecule cm^{-3}), demonstrating that the reaction $CH_3SCH_2O + O_2$ was of negligible importance in our experiments; hence this reaction is not included in the kinetic model. The values of k_4 and Φ(4a) were adjusted until the profiles matched both the H_2CO and HCl data. An example of a typical fit is given in Fig. 5.

Owing to the complexity of the chemical system and uncertainties in some of the rate coefficients, a discussion justifying the choice of rate coefficient values and the sensitivity of the fitted model parameters, k_4 and Φ(4a), to these choices is in order. The results were essentially independent of k_3, k_7 and k_8. The 298 K, 20 Torr rate coefficient and HCl yield for reaction (13) have previously been determined in our laboratory.[17] The first-order loss rates for HCl and H_2CO in our system, k_9 and k_{10}, were measured in a set of experiments using the reaction Cl + CH_3OH in the presence of oxygen as the source of H_2CO and HCl. The value of k_{11} was estimated based on the

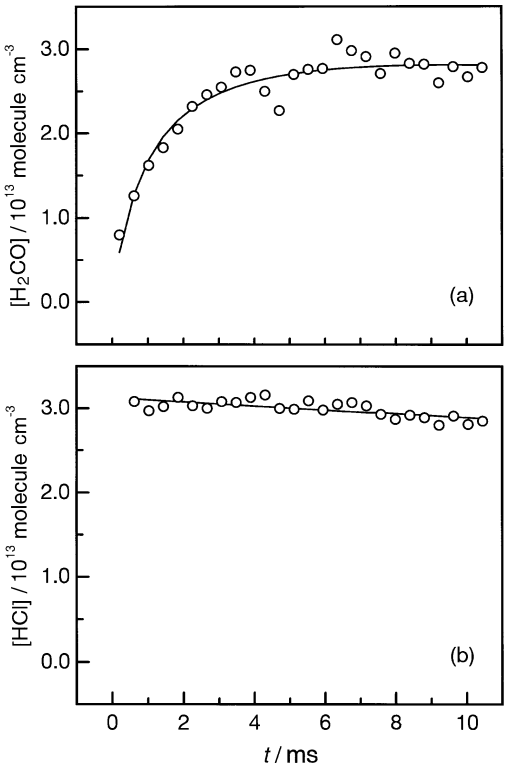

Fig. 5 Typical observed H_2CO and HCl concentration profiles and non-linear least-squares fits using FACSIMILE (see text) for the $CH_3SCH_2O_2$ self-reaction. The fit values for this experiment are Φ(4a) = 1.07 and $k_4 = 1.53 \times 10^{-11}$ cm^3 molecule^{-1} s^{-1}. Experimental conditions: $T = 298$ K; $P = 20$ Torr N_2; concentrations in units of 10^{13} molecule cm^{-3} are 510 DMS + 24 000 O_2 + 4.1 Cl at $t = 0 + 0.3$ photolyzed DMS. The DMS + Cl reaction results in an HCl appearance rate in excess of 1×10^6 s^{-1} which is not resolvable under the experimental conditions employed; thus the fit to the HCl data represents first-order HCl loss only.

Table 1 Kinetic model employed in initial attempts to determine the rate coefficient and H_2CO yield from the $CH_3SCH_2O_2$ self-reaction at 298 K and 20 Torr total pressure

reaction	rate coefficient /cm^3 molecule^{-1} s^{-1}
$Cl_2CO + h\nu \rightarrow 2Cl + CO$ (12)	Φ(Cl) = 2.0[a]
$Cl + DMS \rightarrow HCl + CH_3SCH_2$ (13a)	1.8×10^{-10} [b]
$\rightarrow$ products (13b)	5.0×10^{-11} [b]
$CH_3SCH_2 + O_1(+M) \rightarrow CH_3SCH_2O_2$ (1)	1.0×10^{-12} [c]
$CH_3SCH_2 + CH_3SCH_2 \rightarrow$ products (7)	3.0×10^{-11} [d]
$CH_3SCH_2 + CH_3SCH_2O_2 \rightarrow 2CH_3SCH_2O$ (8)	5.0×10^{-11} [e]
$CH_3SCH_2O_2 + CH_3SCH_2O_2 \rightarrow 2CH_3SCH_2O + O_2$ (4a)	vary
$\rightarrow CH_3SCHO + CH_3SCH_2OH + O_2$ (4b)	vary
$CH_3SCH_2O(+M) \rightarrow H_2CO + CH_3S$ (3)	1×10^5 [f,g]
$HCl \rightarrow$ loss (9)	13[h]
$H_2CO \rightarrow$ loss (10)	11[h]
$CH_3SCH_2O_2 \rightarrow$ loss (11)	5[i]

[a] Ref. 17 and 21; [b] ref. 17; [c] estimate based on ref. 13 and 14; [d] ref. 13; [e] estimate based on analogous R + RO_2 reactions, ref. 30; [f] units s^{-1}; [g] lower limit based on present work (see text); [h] measured in present work; [i] estimate based on measured values of k_9 and k_{10}.

measured values of k_9 and k_{10}. Best fit values for k_4 and Φ(4a) were found to vary by only 10% when the value of k_1 was varied over the range 2.0×10^{-13}–6.0×10^{-11} cm^3 molecule^{-1} s^{-1}. There are two published room-temperature rate coefficients for reaction (1). Butkovskaya and LeBras[14] report a value of 2.0×10^{-13} cm^3 molecule^{-1} s^{-1} in 1 Torr of He and Wallington *et al.*[13] report a value of 5.7×10^{-12} cm^3 molecule^{-1} s^{-1} in 750 Torr of SF_6. Based on these two measurements, the value of k_1 in the present study almost certainly falls within the range of 2.0×10^{-13}–6×10^{-12} cm^3 molecule^{-1} s^{-1}.

Our sensitivity analysis demonstrates that the kinetic model employed to determine the $CH_3SCH_2O_2$ self-reaction rate coefficient and the H_2CO yield from the self-reaction is insensitive to the chosen values of rate coefficients not measured in our laboratory, over the ranges of their reasonable potential values. Fig. 6 shows results thus obtained for the rate coefficient and H_2CO yield of reaction (4). The abscissa in Fig. 6 is the initial concentration of DMS molecules photolyzed by the excimer laser flash assuming an absorption cross-section of 1.28×10^{-20} cm^2 at 248 nm[26] and a 100% dissociation efficiency. The H_2CO yield varies with the DMS photoproduct concentration, causing the observed value to exceed unity in most cases; possible explanations for this observation involving secondary radical–radical reactions are considered below. By extrapolation of the results in Fig. 6 to zero photolysis of DMS, we obtain an H_2CO yield of 0.97 ± 0.08 (2σ, precision only). The extrapolated rate coefficient is $(1.5 \pm 0.2) \times 10^{-11}$ cm^3 molecule^{-1} s^{-1}, which is indistinguishable from a simple average of the observed values (see Fig. 6); due to possible chemistry complications (see below) we consider this rate coefficient an upper limit value.

The dependence of the H_2CO yield on the concentration of DMS photoproducts and the fact that the excess H_2CO is

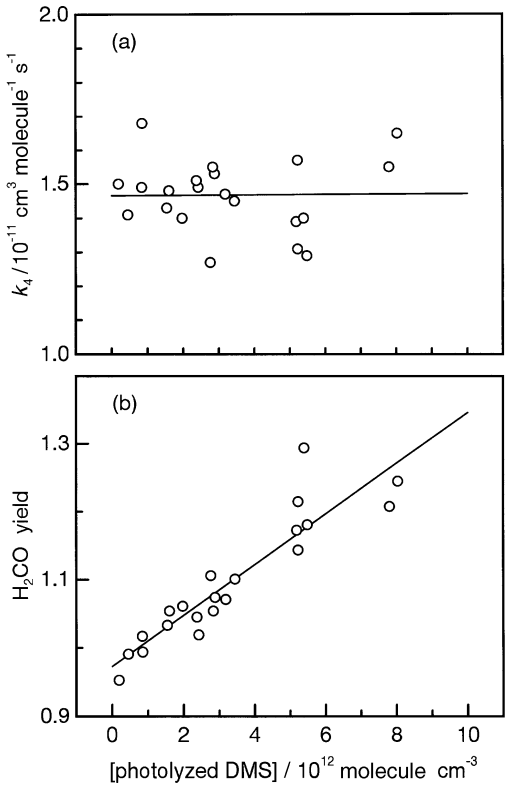

Fig. 6 Results of the study of the $CH_3SCH_2O_2$ self-reaction at $T = 298$ K and $P = 20$ Torr N_2: (a) observed rate coefficient as a function of the concentration of photolyzed DMS; (b) observed H_2CO yield as a function of the concentration of photolyzed DMS. Linear extrapolation to zero concentration of DMS photoproducts gives a yield of 0.97 ± 0.08 where the uncertainty is 2σ and represents precision only.

typically nearly equal to the concentration of DMS molecules photolyzed, suggests that secondary chemistry involving the DMS photoproducts CH_3 and CH_3S is responsible for generating the excess H_2CO. In order to assess the potential importance of complicating secondary chemistry in our experiments, an exhaustive series of numerical simulations was conducted using the ACUCHEM program.[27] These simulations employed the kinetic model listed in Table 1 and the following additional chemistry:

$$CH_3 + O_2 + M \rightarrow CH_3O_2 + M \quad (14)$$

$$CH_3S + CH_3S + M \rightarrow CH_3SSCH_3 + M \quad (15)$$

$$CH_3O_2 + CH_3S \rightarrow CH_3SO + CH_3O \quad (16)$$

$$CH_3SCH_2O_2 + CH_3O_2 \rightarrow CH_3SCH_2O + CH_3O + O_2 \quad (17)$$

$$CH_3SCH_2O_2 + CH_3S \rightarrow CH_3SCH_2O + CH_3SO \quad (18)$$

$$CH_3O + O_2 \rightarrow H_2CO + HO_2 \quad (19)$$

$$CH_3O + CH_3O \rightarrow H_2CO + CH_3OH \quad (20)$$

The rate coefficients for reactions (14),[21] (15),[28,29] (19),[21] and (20)[30,31] were taken from the literature. To our knowledge no kinetic or mechanistic information regarding reactions (17) and (18) is available in the literature. Reaction (16) has been previously proposed by Barnes *et al.*,[32] who observed evidence for its occurrence in chamber studies investigating the NO_x-free photoxidation of dimethyl disulfide; however these authors do not give an estimate of the rate coefficient. While it is possible that reaction (17) proceeds *via* multiple channels, we have only considered the channel with the greatest potential for impacting our experiments.

The series of numerical simulations consisted of sets of simulations generated using the following procedure:

(1) k_4, k_{16}, k_{17} and k_{18} were each assigned a value. (2) A set of numerical simulations was conducted employing initial reactant concentrations equal to those in several of the actual experiments. (3) The H_2CO and HCl concentration profiles generated for each simulation were then analyzed in the same manner as for the data obtained in the experiments; the kinetic model in Table 1 and the FACSIMILE[25] program were employed to adjust the rate coefficient, k_4 and the H_2CO yield, Φ(4a), to fit the simulated concentration profiles. (4) Using the results obtained employing the FACSIMILE[25] program and the kinetic model in Table 1, two sets of data were generated: k_4 and Φ(4a) *vs.* the initial concentration of DMS photoproducts.

Steps (1)–(4) were carried out for 66 different combinations of k_4, k_{16}, k_{17} and k_{18}. The individual values of k_4, k_{16}, k_{17} and k_{18} were varied over the following ranges (units are cm^3 molecule^{-1} s^{-1}): k_4: 0–1.6×10^{-11}; k_{16}: 0–1.0×10^{-10}; k_{17}: 0–1.0×10^{-10}; k_{18}: 0–1.0×10^{-10}.

The two data sets obtained for each combination of k_4, k_{16}, k_{17} and k_{18} were compared with the experimental data to determine if the simulated data were consistent with the two sets of observed data. In particular, the simulated data sets were examined for the following features: (1) a dependence of the H_2CO yield on the initial concentration of photolyzed DMS molecules that was similar to that exhibited by the observed data set and rendered an H_2CO yield of approximately unity when extrapolated to zero DMS photolysis products; (2) an invariance of k_4 with respect to the initial concentration of photolyzed DMS and an average k_4 value that was within two standard deviations of the k_4 average of the observed data set, *i.e* $(1.3–1.7) \times 10^{-11}$ cm^3 molecule^{-1} s^{-1}. All the simulated data sets exhibited some dependence of k_4 on the initial concentration of photolyzed DMS. This is not surprising considering the noise-free nature of the numerical simulations. If the difference between the extreme values of k_4 in a particular data set exceeded the standard deviation of the

observed data set by more than a factor of two then the dependence of k_4 on the initial concentration of photolyzed DMS was considered statistically significant compared to the variability of k_4 in the observed data set and was thus rejected.

Based on the comprehensive battery of numerical simulations described above, we have concluded that secondary chemistry involving CH_3S and CH_3 radicals generated *via* DMS photolysis and CH_3S radicals produced by the decomposition of CH_3SCH_2O may have made a limited contribution to the $CH_3SCH_2O_2$ disappearance kinetics observed in our experiments. Our results indicate that the true value of the $CH_3SCH_2O_2$ self-reaction rate coefficient lies within the range $(1.2 \pm 0.5) \times 10^{-11}$ cm^3 molecule^{-1} s^{-1}.

It is worth noting that the secondary chemistry discussed above could not have affected the results of our study of the $CH_3SCH_2O_2 + NO$ reaction. This is because peroxyl radical concentrations were far too low for these species to compete with NO for consumption of $CH_3SCH_2O_2$ under the experimental conditions employed, and because CH_3S was efficiently scavenged by NO.

The experiments focusing on the $CH_3SCH_2O_2$ self-reaction have demonstrated that this reaction, like the $CH_3SCH_2O_2 + NO$ reaction, produces H_2CO, and hence CH_3S, in approximately unit yield, presumably *via* the decomposition of the unstable CH_3SCH_2O intermediate. The room-temperature rate coefficient for the self-reaction is surprisingly fast, $(1.2 \pm 0.5) \times 10^{-11}$ cm^3 molecule^{-1} s^{-1}. This result is somewhat higher than the value of $(7.9 \pm 1.4) \times 10^{-12}$ cm^3 molecule^{-1} s^{-1} reported by Wallington *et al.*[13] from their observation of $CH_3SCH_2O_2$ disappearance. As in our study, Wallington *et al.*[13] note that the rate coefficient observed in their study may not be the true $CH_3SCH_2O_2$ self-reaction rate coefficient. Wallington *et al.*[13] suggest that complicating secondary chemistry, in particular the $CH_3SCH_2O_2 + CH_3S$ reaction, may have contributed to the observed $CH_3SCH_2O_2$ decay.

Conclusions

We have demonstrated that the reaction of $CH_3SCH_2O_2$ with NO, as well as the $CH_3SCH_2O_2$ self-reaction, produce H_2CO and CH_3S in high yield, and that reaction of the CH_3SCH_2O intermediate with O_2 does not compete with its decomposition under our experimental conditions. However, the certainty of our findings with respect to atmospheric conditions is a bit more tenuous. We have demonstrated that the lifetime of the CH_3SCH_2O intermediate is less than 30 μs at 261 K and 10 Torr total pressure. If k_3, the rate coefficient for CH_3SCH_2O decomposition, is assumed to have a value of *ca.* 35 000 s^{-1} at atmospheric pressure and room temperature (probably a poor assumption) then in 1 atm of air the $CH_3SCH_2O + O_2$ rate coefficient need only be *ca.* 7×10^{-15} cm^3 molecule^{-1} s^{-1} in order to compete equally with CH_3SCH_2O decomposition. Analogous $RO + O_2$ reactions have room-temperature rate coefficients of 1.9×10^{-15} cm^3 molecule^{-1} s^{-1} for $R = CH_3$ and 1.0×10^{-14} cm^3 molecule^{-1} s^{-1} for $R = C_2H_5$.[21] It is thus not out of the question that the reaction $CH_3SCH_2O + O_2$ could be important in the atmospheric oxidation of CH_3SCH_2. However, because the upper limit placed on the CH_3SCH_2O lifetime by our experiments is for 10 Torr total pressure and 261 K, it is highly probable that at atmospheric pressure and temperatures more typical of the lower troposphere, the CH_3SCH_2O lifetime is significantly less than 30 μs. Additionally, while most of the CH_3S yield experiments of Turnipseed *et al.*[11] were conducted in 22 Torr of O_2, they also conducted some experiments in 200 Torr O_2 and saw no indications of a $CH_3SCH_2O + O_2$ reaction producing HO_2. However, owing to the complexity of their experimental technique for inferring HO_2 production, they were not able to rule out unequivocally the possibility of the $CH_3SCH_2O + O_2$ reaction occurring to some degree. Nevertheless, both their results and ours provide strong evidence supporting the notion that, under atmospheric conditions, the fate of the CH_3SCH_2O intermediate is decomposition to CH_3S and H_2CO, as opposed to reaction with molecular oxygen.

A complete picture detailing the fate of CH_3SCH_2 radicals for the range of tropospheric conditions still requires detailed knowledge of other potentially important reactions involving the $CH_3SCH_2O_2$ radical. In particular, reaction with HO_2 may be important. To our knowledge, there exist no published measurements of the rate coefficient for the reaction of $CH_3SCH_2O_2$ with HO_2. Based on analogy with the reactions of alkyl peroxyl radicals with HO_2, one may estimate that the room-temperature rate coefficient for the $CH_3SCH_2O_2 + HO_2$ reaction is of the order of 1×10^{-11} cm^3 molecule^{-1} s^{-1}.[22–24] A reasonable remote marine boundary layer diurnally averaged HO_2 concentration may be *ca.* 1×10^8 molecule cm^{-3} [33] although, of course, actual HO_2 mixing ratios in the marine boundary layer will vary widely as a function of solar flux, water vapour, temperature, and the concentrations of various radical and non-radical species. Using the aforementioned HO_2 concentration and rate coefficient one may roughly estimate the remote marine boundary layer lifetime of $CH_3SCH_2O_2$ with respect to reaction with HO_2 to be of the order of 1000 s. Assuming a typical remote marine boundary layer NO mixing ratio of 5 pptv,[15] the lifetime of $CH_3SCH_2O_2$ with respect to reaction with NO is *ca.* 700 s. Therefore, it is entirely possible that in the marine boundary layer these two reaction pathways are competitive. This is an important point, as the product of the $HO_2 + CH_3SCH_2O_2$ reaction is likely a hydroperoxide (CH_3SCH_2OOH) that would be susceptible to heterogeneous removal from the atmosphere *via* condensation on pre-existing aerosols and cloud droplets as well as deposition at the ocean surface. Thus, $CH_3SCH_2O_2$ reaction with HO_2 may be part of an efficient process that removes volatilized sulfur from the atmosphere, precluding its participation in aerosol and cloud-formation processes that may impact the earth's radiation budget.

Typically, the self reactions of peroxyl radicals other than HO_2 and CH_3O_2 are unimportant in the atmosphere. However, given the rather fast rate coefficient for the $CH_3SCH_2O_2$ self-reaction and the low NO levels typical of the remote marine boundary layer, it is not out of the question that this reaction could be important under certain conditions. An accurate assessment of this reaction's potential atmospheric importance is highly dependent on understanding the kinetics of the $CH_3SCH_2O_2 + HO_2$ reaction.

The present laboratory study, when combined with other recent studies,[11,13] demonstrates that the atmospheric oxidation of the CH_3SCH_2 radical will produce the key species CH_3S in near unit yield, given the absence of competing reactions, such as $CH_3SCH_2O_2 + HO_2$. In the light of the preceeding discussion, it is apparent that laboratory experiments designed to assess the kinetics and mechanism of the $CH_3SCH_2O_2 + HO_2$ reaction should be considered a high priority.

This research was supported by the National Science Foundation under grant number ATM-94-12237. Shawn P. Urbanski was supported by the NASA Earth System Science Fellowship Program. We would like to thank Tim Wallington for insightful comments and suggestions.

References

1 H. Berresheim, P. H. Wine and D. D. Davis, in: *Composition, Chemistry and Climate of the Atmosphere*, ed. H. B Singh, Van Nostrand Reinhold, New York, 1995, pp. 251–307, and references therein.

2 T. S. Bates, B. K. Lamb, A. Guenther, J. Dignon and R. E. Stoiber, *J. Atmos. Chem.*, 1992, **14**, 315.
3 P. A. Spiro, D. J. Jacob and J. A. Logan, *J. Geophys. Res.*, 1992, **97**, 6023.
4 G. E. Shaw, *Climatic Change*, 1983, **5**, 297.
5 R. J. Charlson, J. E. Lovelock, M. O. Andreae and S. G. Warren, *Nature* (*London*), 1987, **326**, 655.
6 G. S. Tyndall and A. R. Ravishankara, *Int. J. Chem. Kinet.*, 1991, **23**, 483.
7 A. J. Hynes, P. H. Wine and D. H. Semmes, *J. Phys. Chem.*, 1986, **90**, 4148.
8 A. J. Hynes, R. B. Stoker, A. J. Pounds, T. McKay, J. D. Bradshaw, J. M. Nicovich and P. H. Wine, *J. Phys. Chem.*, 1995, **99**, 16 967.
9 S. B. Barone, A. A. Turnipseed and A. R. Ravishankara, *J. Phys. Chem.*, 1996, **100**, 14 694.
10 R. E. Stickel, Z. Zhao and P. H. Wine, *Chem. Phys. Lett.*, 1993, **212**, 312.
11 A. A. Turnipseed, S. B. Barone and A. R. Ravishankara, *J. Phys. Chem.*, 1996, **100**, 14 703.
12 H. Niki, P. D. Maker, C. M. Savage and L. P. Breitenbach, *Int. J. Chem. Kinet.*, 1983, **22**, 647.
13 T. J. Wallington, T. Ellermann and O. J. Nielsen, *J. Phys. Chem.*, 1993, **97**, 8442.
14 N. I. Butkovskaya and G. Le Bras, *J. Phys. Chem.*, 1994, **98**, 2582.
15 H. B. Singh, D. Herlth, R. Kolyer, L. Salas, J. D. Bradshaw, S. T. Sandholm, D. D. Davis, J. Crawford, Y. Kondo, M. Koike, R. Talbot, G. L. Gregory, G. W. Sachse, E. Browell, D. R. Blake, F. S. Rowland, R. Newell, J. Merrill, B. Heikes, S. C. Liu, P. J. Crutzen and M. Kanakidou, *J. Geophys. Res.*, 1996, **101**, 1793.
16 D. D. Davis, J. D. Bradshaw, M. O. Rodgers, S. T. Sandholm and S. KeSheng, *J. Geophys. Res.*, 1987, **92**, 2049.
17 R. E. Stickel, J. M. Nicovich, S. Wang, Z. Zhao and P. H. Wine, *J. Phys. Chem.*, 1992, **96**, 9875.
18 Z. Zhao, R. E. Stickel and P. H. Wine, *Chem. Phys. Lett.*, 1996, **251**, 59.
19 S. B. Barone, A. A. Turnipseed, T. Gierczak and A. R. Ravishankara, *J. Phys. Chem.*, 1994, **98**, 11 969.
20 H.-H. Grotheer, G. Riekert, D. Walter and T. Just, *J. Phys. Chem.*, 1988, **92**, 4028.
21 W. B. DeMore, S. P. Sander, D. M. Golden, R. F. Hampson, M. J. Kurylo, C. J. Howard, A. R. Ravishankara, C. E. Kolb and M. J. Molina, *Chemical Kinetics and Photochemical Data for Use in Stratospheric Modeling*; JPL Publication 94-26: Jet Propulsion Laboratory, Pasadena, CA, 1994.
22 R. Atkinson, D. L. Baulch, R. A. Cox, R. F. Hampson Jr., J. A. Kerr and J. Troe, *J. Phys. Chem. Ref. Data*, 1992, **21**, 1125.
23 P. D. Lightfoot, R. A. Cox, J. N. Crowley, M. Destriau, G. D. Hayman, M. E. Jenkin, G. K. Moortgat and F. Zabel, *Atmos. Environ. A*, 1992, **26**, 1805.
24 T. J. Wallington, P. Dagaut and M. J. Kurylo, *Chem. Rev.*, 1992, **92**, 667.
25 A. M. Malleson, H. M. Kellett, R. G. Myhill and W. P. Sweetenham, A.E.R.E. Harwell Publication R 13729, AERE Harwell Publications Office, Oxfordshire, U.K. 1990.
26 C. H. Hearn, E. Turcu and J. A. Joens, *Atmos. Environ. A*, 1990, **24**, 1939.
27 W. Braun, J. T. Herron and D. K. Kahaner, *Int. J. Chem. Kinet.*, 1988, **20**, 51.
28 F. Domine, T. P. Murrels and C. J. Howard, *J. Phys. Chem.*, 1990, **94**, 5839.
29 C. Anastasi, M. Broomfield, O. J. Nielsen and P. Pagsberg, *Chem. Phys. Lett.*, 1991, **182**, 643.
30 W. Tsang and R. F. Hampson, *J. Phys. Chem. Ref. Data*, 1986, **15**, 1087.
31 J. Heicklen, *Adv. Photochem.*, 1988, **14**, 177.
32 I. Barnes, K. H. Becker and N. Milalopoulos, *J. Atmos. Chem.*, 1994, **18**, 267.
33 D. D. Davis, J. Crawford, G. Chen, W. Chameides, S. Liu, J. Bradshaw, S. Sandholm, G. Sachse, G. Gregory, B. Anderson, J. Barrick, A. Bachmeier, J. Collins, E. Browell, D. Blake, S. Rowland, Y. Kondo, H. Singh, R. Talbot, B. Heikes, J. Merrill, J. Rodriguez and R. E. Newell, *J. Geophys. Res.*, 1996, **101**, 2111.

Paper 7/01380I; *Received* 27*th February*, 1997